Regarding the numerical solutions of the Sharma-Tasso-Olver equation

Tukur Abdulkadir Sulaiman[1,2], *Asif* Yokus[3], *Nesrin* Gulluoglu[4,*], and *Haci Mehmet* Baskonus[5]

[1]Department of Mathematics, Firat University, Elazig, Turkey
[2]Department of Mathematics, Federal University, Dutse, Jigawa, Nigeria
[3]Department of Actuary, Firat University, Elazig, Turkey
[4]Department of Mathematics, University of Harran, Sanliurfa, Turkey
[5]Department of Computer Engineering, Munzur University, Tunceli, Turkey

Abstract. With aid of the Wolfram Mathematica package, this study investigates the solutions of a nonlinear model with strong nonlinearity, namely; the Sharma-Tasso-Olver equation. We use the improved Bernoulli sub-equation function method in acquiring the analytical solution to this equation, we successfully obtain one-singular soliton solution with exponential function structure. Through the obtained analytical solution, the finite forward difference method is used in approximating the exact and numerical solutions to this equation. We check the stability of the finite forward difference method with this equation using the Fourier-Von Neumann stability analysis. We find the L_2 and L_∞ norm error to the numerical approximation. We present the interesting 3D and 2D figures of the obtained singular soliton solution. We also plot the graphics of the numerical error, exact and numerical approximations data obtained in this study by using the MATLAB package.

1 Introduction

In the recent decades there has been a rapid development in the search of solutions to the nonlinear evolution equations (NEEs) that arise in the various fields of nonlinear sciences such as physics, biological sciences, chemistry, mathematical physics and engineering. Several scientists have developed various technique for finding solutions to such type of problems [1–19].

However, in this study we investigate the solutions of the Sharma-Tasso-Olver equation [20] by using the improved Bernoulli sub-equation function method (IBSEFM) [21] and the finite forward difference method (FDM) [22]. The Sharma-Tasso-Olver equation:

$$u_t + 3au_x^2 + 3au^2u_x + 3auu_{xx} + au_{xxx} = 0, \tag{1}$$

*Corresponding Author: ngulluoglu@harran.edu.tr

where α is a real constant, u is the unknown function which depends on the temporal variable t and the spatial variable x, $u(x,t)$ describes the wave motion. This equation contains both linear dispersive term and the double nonlinear terms.

Taking $a = 1$ [20], we have

$$u_t + 3u_x^2 + 3u^2 u_x + 3uu_{xx} + u_{xxx} = 0. \tag{2}$$

2 Analysis of IBSEFM

The IBSEFM is developed by extending the Bernoulli sub-equation function method [21]. In the section we present the steps to follow in using the method.

Step 1. Let us consider the following nonlinear partial differential equation;

$$P(u,\ u_x u^2\ u_x,\ u_t,\ \ldots), \tag{3}$$

performing the wave transformation $u(x,\ y,\ z,\ t) = U(\xi)$, $\xi = x + y + z - ct$, reduces Eq. (3) to the following nonlinear ordinary differential equation (NODE);

$$Q(U,\ U^{'}\ U^{''},\ U^3,\ \ldots), \tag{4}$$

Step 2. Consider the following as a trial solution to Eq. (3);

$$U(\xi) = \frac{\sum_{i=0}^{n} a_i G^i}{\sum_{j=0}^{m} b_j G^j} = \frac{a_0 + a_1 G + a_2 G^2 + \ldots + a_n G^n}{b_0 + b_1 G + b_2 G^2 + \ldots + b_m G^m}, \tag{5}$$

according to the Bernoulli theory,

$$G^{'} = wG + dG^M,\ w \neq 0,\ d \neq 0,\ M \in \mathbb{R} \setminus \{0, 1, 2\}, \tag{6}$$

where $F = F(\xi)$ is a Bernoulli differential polynomial. Substituting Eq. (6) into (4) produces an equation of polynomial $\Psi(G)$ function of G:

$$\Psi(G) = \rho_s G^s + \ldots + \rho_1 G + \rho_0. \tag{7}$$

We obtain the values of n, m and M by using the balancing technique.

Step 3. We obtain a system of algebraic equations by letting the summations of every coefficients of $\Psi(G)$ with the same power to zero. We obtain the values of the coefficients $a_0, \ldots, a_n$ and $b_0, \ldots, b_n$ by solving the system of equations.

Step 4. Solving the nonlinear Bernoulli differential equation (Eq. (6)), gives the following two cases based on w and d:

$$G(\xi) = \left[\frac{-d}{w} + \frac{\epsilon}{e^{w(M-1)\xi}}\right]^{\frac{1}{1-M}}, \quad w \neq d \tag{8}$$

$$G(\xi) = \left[\frac{(\epsilon - 1) + (\epsilon + 1)tanh\left(\frac{w(1-M)\xi}{2}\right)}{1 - tanh\left(\frac{w(1-M)\xi}{2}\right)}\right]^{\frac{1}{1-M}}, \quad w = d, \epsilon \in \mathbb{R}. \tag{9}$$

Using the complete discrimination of the polynomial of G, we solve the algebraic system of equations with the help of Wolfram Mathematica 9 and obtain the various

cases for the results of the coefficients. We obtain the exact solutions to Eq. (3) by substituting the obtained values of the coefficients into the trial solution that is Eq. (5).

3 The Analysis of FDM

Presenting the analysis of the finite forward difference method needs the following notations;

1. Δx which is the spatial step
2. Δt which is the time step
3. $x_i = a + i\Delta x$, $i = 0, 1, 2, ..., N$ stands for the coordinates points of mesh and $N = \frac{b-a}{\Delta x}$, $t_j = j\Delta x$, $j = 0, 1, 2, ..., M$ and $M = \frac{T}{\Delta t}$.
4. the function $u(x,t)$ stands for the values of these solutions at the grid points which is $u(x_i, t_j) \approx u_{i,j}$.
5. the $u_{i,j}$ represent the numerical approximatios of the exact values of $u(x,t)$ at the point (x_i, t_j)

We then collect the following finite forward difference operators:

$$H_t u_{i,j} = u_{i,j+1} - u_{i,j}, \tag{10}$$

$$H_x u_{i,j} = u_{i+1,j} - u_{i,j}, \tag{11}$$

$$H_{xx} u_{i,j} = u_{i+1,j} - 2u_{i,j} + u_{i-1,j}. \tag{12}$$

$$H_{xxx} u_{i,j} = u_{i+2,j} - 2u_{i+1,j} + 2u_{i-1,j} - u_{i-2,j}. \tag{13}$$

We the give the approximate forms of the partial derivatives for the difference operators as:

$$\left.\frac{\partial u}{\partial t}\right|_{i,j} = \frac{H_t u_{i,j}}{\Delta t} + O((\Delta t)), \tag{14}$$

$$\left.\frac{\partial u}{\partial x}\right|_{i,j} = \frac{H_x u_{i,j}}{\Delta x} + O((\Delta x)), \tag{15}$$

$$\left.\frac{\partial^2 u}{\partial x^2}\right|_{i,j} = \frac{H_{xx} u_{i,j}}{(\Delta x)^2} + O((\Delta x)^2), \tag{16}$$

$$\left.\frac{\partial^3 u}{\partial x^3}\right|_{i,j} = \frac{H_{xxx} u_{i,j}}{(\Delta x)^3} + O((\Delta x)^2), \tag{17}$$

Eq. (2) may be written in the finite difference operator form as:

$$\frac{H_t u_{i,j}}{\Delta t} + 3\Big(\frac{H_x u_{i,j}}{\Delta x}\Big)^2 + 3u_{i,j}^2 \frac{H_x u_{i,j}}{\Delta x} + 3u_{i,j} \frac{H_{xx} u_{i,j}}{(\Delta x)^2} + \frac{H_{xxx} u_{i,j}}{(\Delta x)^3} = 0. \tag{18}$$

Inserting Eqs. (10), (11), (12) and (13) into Eq. (18), yields the following indexed form:

$$u_{i+1,j} = \frac{1}{6}\Bigg(\frac{1}{(\Delta x)} + 6u_{i,j} - 3(\Delta x)u_{i,j}^2 - \frac{1}{\sqrt{(\Delta t)}(\Delta x)}\Big((\Delta t) + 6(\Delta t)(\Delta x)u_{i-2,j} - 12(\Delta t)(\Delta x)u_{i-1,j} + 12(\Delta t)(\Delta x)u_{i,j} + 12(\Delta x)^4 u_{i,j} - 36(\Delta t)(\Delta x)^2 u_{i-1,j}u_{i,j} + u_{i,j} + 66(\Delta t)(\Delta x)^2 u_{i,j}^2 + 9(\Delta t)(\Delta x)^4 u_{i,j}^4 - 12(\Delta x)^4 u_{i,j+1} - 36(\Delta t)(\Delta x)^2 u_{i,j}u_{i,j+1} - 6(\Delta t)(\Delta x)u_{i+2,j}\Big)^{\frac{1}{2}}\Bigg). \tag{19}$$

Remark-1: We consider $u_{i,0} = u_0(x_i)$ as initial value.

4 Application of IBSEFM

In this section, we employ the IBSEFM in searching for the solutions of the Sharma-Tasso-Olver equation given in Eq. (2).

Using the wave transformation $u = U(\xi)$, $\xi = x - kt$ on Eq. (2), gives the following NODE;

$$U^3 - kU + 3UU^{'} + U^{''} = 0. \tag{20}$$

We apply the balancing technique to Eq. (20) there by using the highest power nonlinear term U^3 and the highest derivative $U^{''}$, we therefore obtain this relation $n + 1 = M + m$. Choosing $M = 3$ and $m = 1$, we get $n = 3$.

We may therefore write the following equation by using Eq. (5) along with $m = 1$ and $n = 3$;

$$U(\xi) = \frac{a_0 + a_1G(\xi) + a_2G^2(\xi) + a_3G^3(\xi)}{b_0 + b_1G(\xi)} = \frac{\Phi}{\Omega}, \tag{21}$$

differentiating Eq. (21) for the first and the second time, we have the following equations;

$$U^{'}(\xi) = \frac{\Phi^{'}(\xi)\Omega(\xi) - \Phi(\xi)\Omega^{'}(\xi)}{\Omega^2(\xi)}, \tag{22}$$

$$U^{''}(\xi) = \frac{\Phi^{''}(\xi)\Omega(\xi) - \Phi(\xi)\Omega^{'}(\xi)}{\Omega^2(\xi)} - \frac{[\Phi(\xi)\Omega^{'}(\xi)]^{'}\Omega^2(\xi) - 2\Phi(\xi)[\Omega^{'}(\xi)]^2\Omega(\xi)}{\Omega^4(\xi)}, \tag{23}$$

where $G^{'} = wG + dG^3$, $w \neq 0$, $d \neq 0$. Substituting Eq. (22) and (23) into Eq. (20) and simplifying, we obtain an equation that involves the polynomials of G. We therefore collect the system of equations there by equating the summation of the coefficients of G that are having the same power to zero. We solve the system of equations with the help of Wolfram Mathematica 9 and obtain the following case;

Case-1: For $w \neq d$, we have

Case-1.1:

$$a_0 = -2wb_0, a_1 = -2wb_1, a_2 = -4db_0, a_3 = -4db_1, k = 4w^2$$

,

substituting these coefficients into Eq. (21), we obtain the following singular soliton solution to Eq. (2)

$$u(x,\ t) = 2w\left(1 + \frac{2\epsilon w}{de^{2w(x-4w^2t)} - \epsilon w}\right). \tag{24}$$

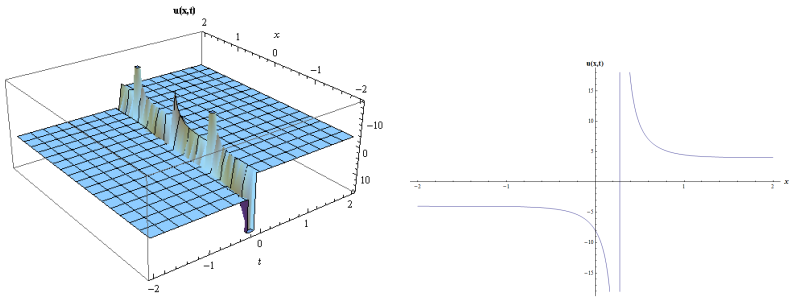

Figure 1. The singular soliton surface of Eq. (24) by substituting the values $w = 2$, $d = 0.2$, $\epsilon = 0.3$, $-13 < x < 13$, $-2 < t < 2$ and $t = 0.0000001$ for the 2D graphic.

5 Von-Neumann Stability Analysis

In this section, we utilize the Von-Neumann stability analysis in investigating the stability of the the finite forward difference method with Eq. (2). We consider ξ^n to be the amplication factor. The growth factor of a typical Fourier mode is therefore defined as:

$$u_m^n = \xi^n e^{im\Phi}, \tag{25}$$

where $i = \sqrt{-1}$.

The Sharma-Tasso-Olver equation is an equation with strong nonlinearity. To check the stability of the numerical scheme, the nonlinear terms u_x^2, u^2u_x and uu_x in Eq. (2) are linearized by making the quantity $\widehat{u_1} = 3u_x$, $\widehat{u_2} = 3u^2$ and $\widehat{u_3} = 3u$ the local constants. Thus, the nonlinear terms $3u_x^2$, $3u^2u_x$ and $3uu_{xx}$ in Eq. (2) become $\widehat{u_1}u_x$, $\widehat{u_2}u_x$ and $\widehat{u_3}u_{xx}$ respectively. In this case Eq. (2) becomes

$$u_t + \widehat{u_1}u_x + \widehat{u_2}u_x + \widehat{u_3}u_{xx} + u_{xxx} = 0. \tag{26}$$

Putting Eq. (14), (15), (16), (17) and Eq. (25) into Eq. (26), hence we get:

$$\xi = X + iY, \tag{27}$$

wnere

$$X = \frac{1}{((\Delta x)^2 + (\Delta t)\widehat{u_3})}\Big((\Delta x)^2 + (\Delta x)(\Delta t)\widehat{u_1} + (\Delta x)(\Delta t)\widehat{u_2} + 2(\Delta t)\widehat{u_3} \\ -(\Delta x)(\Delta t)\widehat{u_1}cos(\Phi) - (\Delta x)(\Delta t)\widehat{u_2}cos(\Phi) - (\Delta t)\widehat{u_3}cos(\Phi)\Big) \tag{28}$$

and

$$Y = -\frac{(\Delta t)sin(\Phi)}{(\Delta x)((\Delta x)^2 + (\Delta t)\widehat{u_3})}\Big(- 2 + (\Delta x)^2\widehat{u_1} + (\Delta x)^2\widehat{u_2} - (\Delta x)\widehat{u_3} + 2cos(\Phi)\Big), \tag{29}$$

which imply that

$$|\xi|^2 = X^2 + Y^2. \tag{30}$$

If this implies $|\xi| \leq 1$ conditional, the method is unconditionally stable [23].

Remark-2: The numerical approximation and stability of the numerical scheme with Eq. (2) depend on how small (Δx) and (Δt) are chosen.

6 L_2 and L_∞ Error Norms

We investigate the numerical and exact approximation of the Sharma-Tasso-Olver equation in this study. We show that how numerical and exact approximations are close to each other by using the L_2 and L_∞ error norms. The L_2 and L_∞ error norms can be defined as [22]:

$$L_2 = \left\|u^{exact} - u^{numeric}\right\|_2 = \sqrt{h\sum_{j=0}^{N}\left|u_j^{exact} - u_j^{numeric}\right|^2},$$

$$L_\infty = ||u^{exact} - u^{numeric}||_\infty = \max_j |u_j^{exact} - u_j^{numeric}|.$$

7 Numerical Example

This section presents the numerical and exact approximations obtained from Eq. (2) under the following data $w = 2$, $d = 0.2$, $\epsilon = 0.3$. Inserting these values into Eq. (2), yields the following special exact solution:

$$u(x,t) = 4\left(1 + \frac{1.2}{-0.6 + 0.2e^{4(x-16t)}}\right). \tag{31}$$

A $t = 0$, we get the following equations:

$$u_0(x) = 4\left(1 + \frac{1.2}{-0.6 + 0.2e^{4x}}\right). \tag{32}$$

According to the finite forward difference method, inserting the values $(\Delta x) = (\Delta t) = 0.0000001$ into Eq. (19), yields the following:

$$u_{i+1,j} = 1.0666 \times 10^{-13}\Big(1.5625 \times 10^{19} + 9.375 \times 10^{12}u_{i,j} - 468750u_{i,j}^2 + \Big(2.44141 \times 10^{38} + 1.46484 \times 10^{32}u_{i-2,j} - 2.92969 \times 10^{32}u_{i-1,j} + 2.9296 \times 10^{32}u_{i,j} - 8.78906 \times 10^{26}u_{i,j}^2 + 2.19727 \times 10^{11}u_{i,j}^4 - 2.92964 \times 10^{18}u_{i,j+1} - 8.78906 \times 10^{25}u_{i,j}u_{i,j+1} - 1.46484 \times 10^{32}u_{i+2,j}\Big)^{\frac{1}{2}}\Big). \quad (33)$$

We present in Tables 1 and 2 below, the exact and numerical values and the L_2, L_∞ error norm obtained with the finite forward difference method respectively.

Table 1.

x_i	t_j	Numerical solution	Exact Solution	Eror
0	0.01	-8.00024	-7.99616	4.07756×10^{-5}
0.01	0.01	-8.00048	-7.99640	4.07788×10^{-5}
0.02	0.01	-8.00072	-7.99664	4.07821×10^{-5}
0.03	0.01	-8.00096	-7.99688	4.07853×10^{-5}
0.04	0.01	-8.00120	-7.99712	4.07886×10^{-5}
0.05	0.01	-8.00144	-7.99736	4.07919×10^{-5}
0.06	0.01	-8.00168	-7.99760	4.07951×10^{-5}

Table 1: Numerical and exact solutions of Eq. (2) and absolute errors at $\Delta(x) = \Delta(t) = 0.0000001$ and $0 \leq x \leq 1$ by considering Eq. (31).

Table 2.

$x_i = t_j$	L_2	L_∞
0.001	1.99556×10^{-1}	9.60626×10^{-1}
0.0001	4.20020×10^{-3}	4.39084×10^{-2}
0.00001	1.28802×10^{-4}	4.10969×10^{-3}
0.0000001	1.28378×10^{-7}	4.08043×10^{-5}

Table 2: L_2 and L_∞ error norm when $0 \leq h \leq 1$ and $0 \leq x \leq 1$

Figure 2. Numerical and exact solution of Eq. (3) by considering Eq. (8).

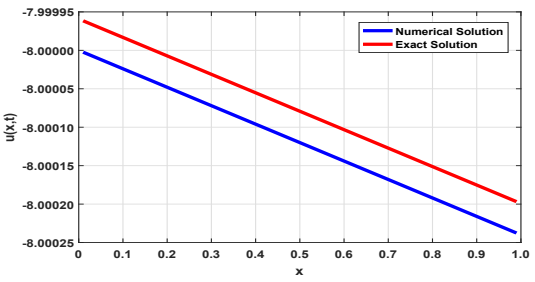

Figure 3. Absolute error graphic at $\Delta(x) = \Delta(t) = 0.0000001$.

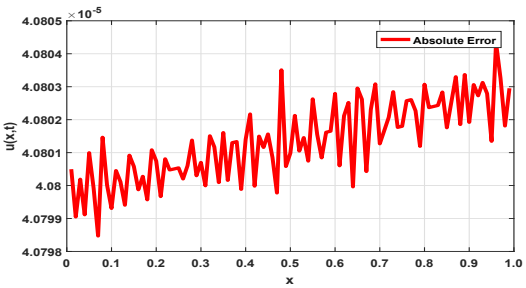

8 Conclusion

I this study, with the aid of the Wolfram Mathematica package, we implemented the improved Bernoulli sub-equation function method in obtaining the analytical solution to the Sharma-Tasso-Olver equation. We successfully obtained one-singular soliton solution in exponential function form. The obtained analytical solution indeed satisfy the considered model. We presented the 2D and 3D graphics of the obtained analytical solution in this study. On the other hand, the finite forward difference scheme is used in approximating the numerical and exact solutions of the considered model. The comparison between exact and numerical approximation is presented in tables 1 and 2 and supported by figure 2 and 3. We observed from figure 2, as Δx approaching 0 the truncation errors are very small, which shows that numerical and exact approximations are coming closer to each other. In summary, the improved Bernoulli sub-equation function method is a powerful and efficient mathematical approach which can be applied to various nonlinear evolution equations and gives a very good results. Furthermore, the analytical solutions obtained by using the improved Bernoulli sub-equation function method can be used to approximate the exact and numerical solutions of various nonlinear evolution equations. To the best of our knowledge this approach is not submitted to literature beforehand.

References

[1] X. Li, International Journal of Differential Equations **2012**, 596762 (2012)
[2] R.I. Nuruddeena, L. Muhammad, A.M. Nass and T.A. Sulaiman, Palestine Journal of Mathematics **7(1)** 262–280 (2018)
[3] T.A. Sulaiman, T. Akturk, H. Bulut and H.M. Baskonus, Journal of Electromagnetic Waves and Applications **32(9)**, 1093–1105 (2017)
[4] H. Bulut, T.A. Sulaiman and B. Demirdag, Nonlinear Dyn. **91** 1985–1991 (2018)
[5] A. Yokus, H.M. Baskonus, T.A. Sulaiman and H. Bulut, Numer Methods Partial Differential Eq. **34**, 211–227 (2018)
[6] Y. Zhao, Journal of Applied Mathematics **2013**, 895760 (2013)
[7] O.A. Ilhan, T.A. Sulaiman, H. Bulut and H.M. Baskonus, Eur. Phys. J. Plus **133**, 27 (2018)
[8] Z. Jin-Ming and Z. Yao-Ming, Chin. Phys. B **21(1)**, 010205 (2011)
[9] H.M. Baskonus, T.A. Sulaiman and H. Bulut, Optik **131**, 1036-1043 (2017)

[10] H. Bulut, T.A. Sulaiman and H.M. Baskonus, Opt. Quant. Electron **48**, 564 (2016)
[11] H. Bulut, T.A. Sulaiman, H.M. Baskonus and A.A. Sandulyak, Optik **135** 327-336 (2017)
[12] S. Momani and S. Abuasad, Chaos, Solitons and Fractals, **27(5)** 1119-1123 (2006)
[13] M. Dehghan and F. Shakeri, Journal of Computational and Applied Mathematics **214**, 435-446 (2008)
[14] O.H. El-Kalaawy, International Journal of Basic and Applied Sciences **3(4)**, 466-478 (2014)
[15] S. Duran, M. Askin and T.A. Sulaiman, IJOCTA **7(3)**, 240–247 (2017)
[16] R. Pourgholi and A. Saeedi, Numer Methods for Partial Differential Equations **33**, 88-104 (2017)
[17] B. Karaagac and A. Esen, Numer Methods for Partial Differential Equations 34(5), 1637-1644 (2018)
[18] O. Omer, A. Esenand F. Bulut, Engineering with Computers 1-12 (2018)
[19] A. Esen, B. Karaagac and O. Tasbozan, Appl. Math. Inf. Sci. Lett 4(1), 1-4 (2016)
[20] I.E. Inan and D. Kaya, Physica A **381** 104-115 (2007)
[21] H. Bulut, H.A. Isik and T.A. Sulaiman, ITM Web of Conferences **13,** 01019 (2017)
[22] A. Yokus, T.A. Sulaiman and H. Bulut, Opt Quant Electron **50**, 31 (2017)
[23] A. Golbabai and E. Mohebianfar, Journal of Nonlinear Science and Applications **49(2)**, 271-288 (2016)